Isoxazolo-[3,4-*d*]-pyridazin-7-(6*H*)-one as a Potential Substrate for New Aldose Reductase Inhibitors

Luca Costantino,[†] Giulio Rastelli,[†] M. Cristina Gamberini,[†] M. Paola Giovannoni,[‡] Vittorio Dal Piaz,[‡] Paola Vianello,[§] and Daniela Barlocco*[,§]

Dipartimento di Scienze Farmaceutiche, Via G. Campi 183, 41100 Modena, Italy, Dipartimento di Scienze Farmaceutiche, Via G. Capponi 9, 50121 Firenze, Italy, and Ist. Chimico Farmaceutico e Tossicologico, Viale Abruzzi 42, 20131 Milano, Italy

Received October 21, 1998

The isoxazolo-[3,4-*d*]-pyridazin-7-(6*H*)-one (**2**) and its corresponding open derivatives 5-acetyl-4-amino-(4-nitro)-6-substituted-3(2*H*)pyridazinones (**3**, **4**) were used as simplified substrates for the synthesis of new aldose reductase inhibitors with respect to the previously reported 5,6-dihydrobenzo[*h*]cinnolin-3(2*H*)one-2 acetic acids (**1**). Moreover, a few derivatives lacking the 5-acetyl group were prepared. Several compounds derived from **2** displayed inhibitory properties comparable to those of Sorbinil. In this class the presence at position 6 of a phenyl carrying an electron-withdrawing substituent proved to be beneficial, independently from its position on the ring (**5g**,**j**−**l**). Acetic acid derivatives were more effective than propionic and butyric analogues. On the contrary, all the monocyclic compounds (**6**−**8**) were either inactive or only weakly active. The 3-methyl-4-(*p*-chlorophenyl)isoxazolo-[3,4-*d*]-pyridazin-7-(6*H*)-one acetic acid (**5g**), which proved to be the most potent derivative, was also investigated in molecular modeling studies, to assess possible similarities in its interaction with the enzyme, with respect to the model **1**.

Introduction

In the western world the incidence of non-insulin-dependent diabetes mellitus (NIDDM) is increasing at an almost epidemic rate. Because of its high incidence and the associated morbidity and mortality, NIDDM has become a major health hazard. No doubt, an important role in the dramatic impact of this disease is represented by the late onset of several complications, namely neuropathy, nephropathy, rethinopathy, and cataract. Though several metabolic pathways have been implicated in the toxic effects of hyperglycaemia,[1] over two decades of intensive studies on several experimental diabetic animal models have demonstrated a link between glucose metabolism via the polyol pathway and diabetic complications.[2,3] Even though numerous clinical trials for the treatment of diabetic neuropathy have been conducted over 16 years, pharmacokinetic problems connected to aldose reductase inhibitors (ARIs) together with the length of trials resulted in the lack of observed efficacy.[4] Thus, there is still a need for new ARIs.

In the course of previous studies[5] we reported the 5,6-dihydrobenzo[*h*]cinnolin-3(2*H*)one-2-acetic acid (**1**) as a model for potent and selective ARIs. Molecular modeling investigations revealed that the carboxylic acid function of **1** binds within a favorable distance with the nicotinamide ring of $NADP^+$ and gives three strong hydrogen bonds with Tyr48, His110, and Trp111.[5] These last residues and the positive nicotinamide ring of $NADP^+$ form a positively charged binding site which is responsible for the binding of negatively charged inhibitors such as the carboxylates.[6,7] In addition, the carbonyl group of the pyridazinone ring of **1** hydrogen bonds to Cys298, while the tricyclic ring gives hydrophobic contacts with other protein residues that constitute the active site.[5] We have now extended our investigations to verify if the tricyclic system is an essential requirement for activity. To this aim, the isoxazolo-[3,4-*d*]-pyridazin-7-(6*H*)-one (**2**)[8] was chosen as a potential new substrate, since, when substituted with an acetic acid side chain at position 6, it still possesses the fundamental pharmacophoric elements disclosed for the model compound **1**, but has the advantages of being a simplified and more versatile substrate to be functionalized. In fact, it can be opened either by reducing or oxidizing agents[8] to give compounds **3** and **4**, respectively, which would offer the possibility to introduce different substituents on the pyridazinone ring. Compound **2** was therefore used both as such and as its monocyclic 4-substituted-5-acetyl **3** and **4** derivatives leading to compounds **5**−**7**. Finally, since the 5-acetyl group proved to interfere with several chemical processes giving unwanted final compounds, a few examples of derivatives lacking it (compounds **8**) were prepared to establish its real importance in the interaction with the enzyme. (See Chart 1)

This paper describes the synthesis of compounds **5**−**8** together with their in vitro ability to inhibit aldose reductase (ALR2). Moreover, molecular modeling of the structure of the complex between aldose reductase and the most active derivative of the new series (**5g**) was performed, and the results were compared with previous modeling data on benzocinnolinones.

Chemistry

Compounds **5** were prepared from the appropriate isoxazolo-[3,4-*d*]-pyridazin-7-(6*H*)-one (**2**)[8] by condensing

* To whom correspondence should be addressed.
[†] Dipartimento di Scienze Farmaceutiche, Modena.
[‡] Dipartimento di Scienze Farmaceutiche, Firenze.
[§] Ist. Chimico Farmaceutico e Tossicologico.

10.1021/jm981107o CCC: $18.00
Published on Web 05/15/1999

Chart 1

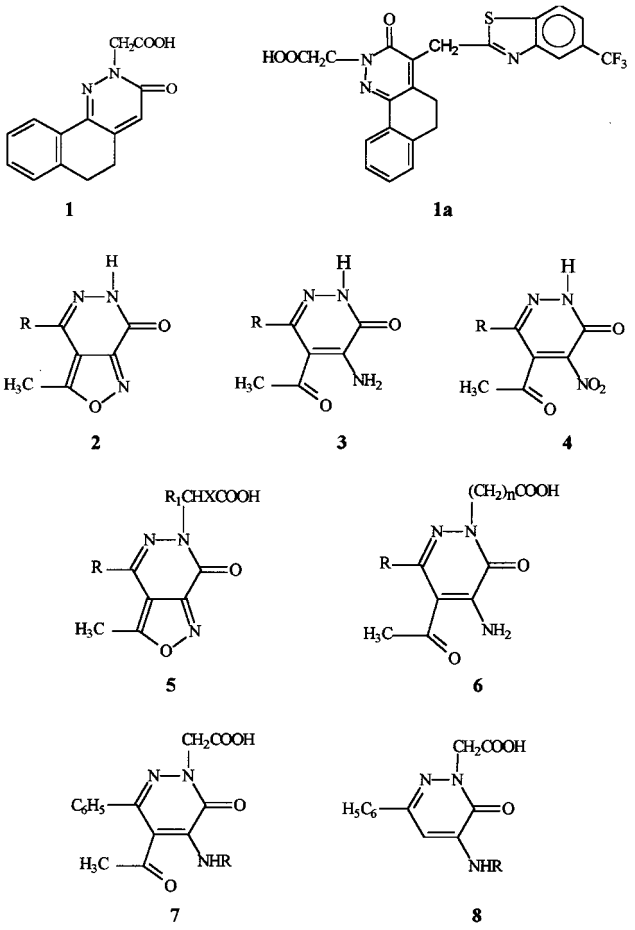

with the required alkyl bromoester to give **9**, easily converted to the desired acids by alkaline hydrolysis. The *p*-NO_2 (**5j**) and the *o*-NO_2 (**5l**) were obtained in a 60/40 mixture by treatment of **5a** with H_2SO_4/HNO_3 and easily separated by flash chromatography. (See Scheme 1.) Compounds **6** were obtained from **3**, in turn prepared from **2**, following literature methods.[8] Attempts to apply to the 6-unsubstituted **2** the oxidative opening above-reported for its methyl analogue always led to a very complex reaction mixture. Compound **2** was therefore first condensed with ethylbromoacetate to give **9a**, which was successfully opened by treatment with ceric ammonium nitrate to **10**. The latter was condensed with the appropriate amine to **11a**−**g** and hydrolyzed as usual to the desired **7a**−**f**. Attempts to introduce the trifluoromethylbenzothiazol-2-yl-methyl-amino moiety, which is known to confer high potency to several aldose reductase inhibitors,[9,10] led to the ester **11g**. However, its hydrolysis was paralleled by an unexpected cyclization giving compound **7g**. (See Scheme 2.) Finally, compounds **8a**−**d** were easily synthesized from the previously reported **13**[11] by formation of the corresponding aminopyridazinones **15** according to literature methods[11] and subsequently substituted at position 2, as described for **5**. (See Scheme 3.)

Results and Discussion

Aldose Reductase Inhibition. The 3-methyl-4-phenylisoxazolo-[3,4-*d*]-pyridazin-7-(6*H*)-one-6-acetic acid (**5a**) showed a capability to inhibit AR fully comparable to

Scheme 1

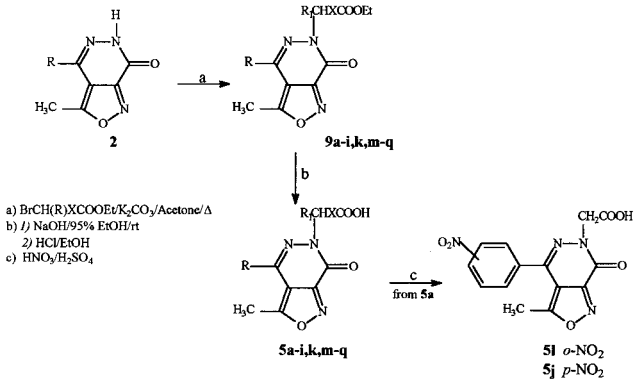

Compd		R	R_1	X
5, 9	**a**	C_6H_5	H	--
	b	C_6H_5	H	CH_2
	c	C_6H_5	H	$(CH_2)_2$
	d	CH_3	H	--
	e	CH_3	H	CH_2
	f	CH_3	H	$(CH_2)_2$
	g	*p*-ClC_6H_4	H	--
	h	*p*-ClC_6H_4	H	CH_2
	i	*p*-ClC_6H_4	H	$(CH_2)_2$
	k	*m*-$NO_2C_6H_4$	H	-
	m	C_6H_5	H	$(CH_2)_3$
	n	C_6H_5	CH_3	--
	o	C_6H_5	CH_2CH_3	--
	p	C_6H_5	$(CH_2)_2CH_3$	--
	q	C_6H_5	H	CH=CH

that of the benzocinnolinone **1** (IC_{50} of 12.72 vs 12.55), thus confirming what was suggested by a theoretical approach. (See modeling studies.) Substitution of the phenyl by a methyl group led to a significantly less active compound (**5e**). On the contrary, insertion of a *p*-chlorine atom gave the most potent derivative (**5g**, $IC_{50} = 3.72\ \mu M$) of the series. A quite similar result was obtained with the more strongly electron-withdrawing nitro group (**5j**, $IC_{50} = 4.76\ \mu M$). Moving the nitro group from para to meta (**5k**, $IC_{50} = 4.46\ \mu M$) and ortho positions (**5l**, $IC_{50} = 6.06\ \mu M$) did not significantly change the potency. Elongation of the acetic acid chain by one methylene decreased the activity on all substrates (**5b,e,h**), in agreement with what was previously seen for the benzocinnolinonic series.[5] Further elongation to butyric (**5c,f,i**) or pentanoic acid (**5m**) partially restored potency. On the contrary, the presence of branched (**5n**−**p**) or unsaturated (**5q**) acidic chains at position 6 was detrimental. (See Table 1.) The opened derivative **6a** was significantly less active than **5a**. The same was true for the higher homologue **6b** and the 6-methyl derivative **6d** with respect to **5d**, thus suggesting the importance of the bicyclic system for a correct orientation of the inhibitors inside the binding pocket of the enzyme. (See Table 2.) Substitution at the amino group of **6a** by a phenyl (**7a**) did not ameliorate its profile, nor did the presence of a *p*-Cl (**7d**) or a *p*-Br (**7e**) on the phenyl ring. On the contrary, insertion on the amino of a benzyl led to a compound significantly more active than **6a** (**7b**, $IC_{50} = 27.60\ \mu M$), though still less potent than the closed model **5a**. Further insertion of an additional methylene (**7c**) again caused loss of activity. (See Table 3.) A few derivatives lacking the 5-acetyl group were also tested. Unfortunately, none of them were found to have significant potency. It should be noted that, as for **7**, also in this series the most

Scheme 2

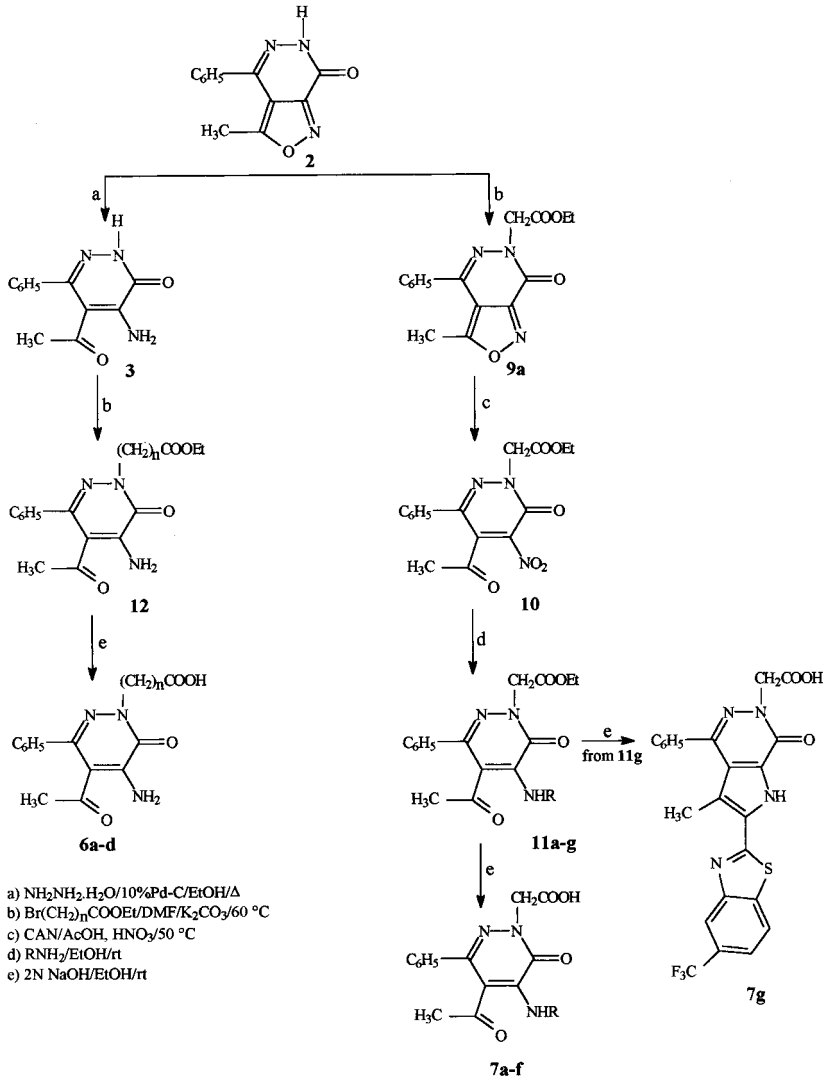

For **7**: R=C_6H_5 **a**; $CH_2C_6H_5$ **b**; $(CH_2)_2C_6H_5$ **c**; *p*-ClC_6H_4 **d**; *p*-BrC_6H_4 **e**; $CH_2C_6H_4Cl$-*p* **f**; [5-(trifluoromethyl)benzothiazol-2-yl]methyl **g**

Scheme 3

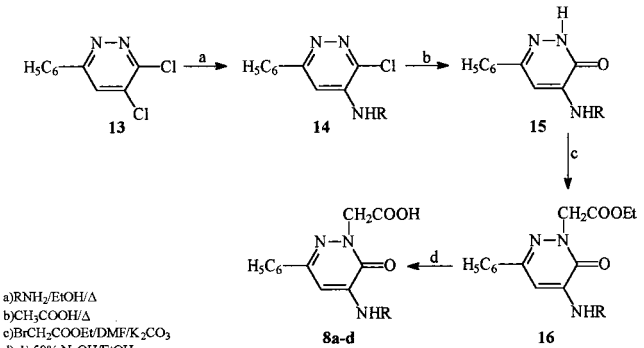

Compd	R	Compd	R
8a	H	**8c**	$CH_2CH_2C_6H_5$
8b	$CH_2C_6H_5$	**8d**	CH_2CH_2-pyridyl-2

significant derivative (**8b**, IC_{50} = 48.82 μM) had a benzyl group at position 4. (See Table 4)

Modeling Studies. In the complexes between ALR2 and the potent inhibitors zopolrestat[6] and tolrestat,[7] an anion binding site particularly suitable for the binding of carboxylates of inhibitors and constituted by Tyr48, His110, and the positive nicotinamide ring of $NADP^+$ was identified. The availability of X-ray crystal structures of ALR2 prompted molecular modeling studies. We have recently docked and energy-minimized a representative member of a new series of benzocinnolinone carboxylic acid inhibitors into the binding site of ALR2,[5] and performed a cycle of structure-based drug design to obtain a new derivative, carrying a benzothiazole substituent at position 4 (compound **1a**), which proved to be a 100-fold better inhibitor.[12] With the aim of investigating the possible analogies between the complexes of ALR2 with previously studied benzocinnolinone carboxylic acid inhibitors[5] and the isoxazolopyridazinone derivatives here reported, we have constructed the complex between ALR2 and the most active derivative of this new series, compound **5g**, in Table 1. Figure 1 illustrates a selection of residues (4 Å) interacting with the inhibitor in the structure of the minimized complex. In agreement with molecular modeling results obtained for the benzocinnolinone carboxylic acid inhibitors,[5,12] the carboxylate of **5g** hydrogen bonds to Tyr48, His110, and Trp111. Moreover, the carbonyl oxygen of the

Table 1. Structural and Biological Properties of Compounds **5a**−**q**

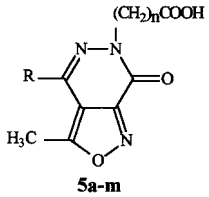

5a-m

compd	R	*n*	yield %[a]	formula[b]	ALR2 inhibition[c]
5a	C_6H_5	1	87	$C_{14}H_{11}N_3O_4$	12.72 (10.34−15.65)
5b	C_6H_5	2	85	$C_{15}H_{13}N_3O_4$	65.17 (50.59−83.96)
5c	C_6H_5	3	88	$C_{16}H_{15}N_3O_4$	20.20 (15.25−26.75)
5d	CH_3	1	75	$C_9H_9N_3O_4$	42.01 (33.99−51.92)
5e	CH_3	2	72	$C_{10}H_{11}N_3O_4$	28% (190 μM)
5f	CH_3	3	70	$C_{11}H_{13}N_3O_4$	65.05 (49.35−85.75)
5g	*p*-ClC_6H_4	1	80	$C_{14}H_{10}ClN_3O_4$	3.72 (2.90−4.63)
5h	*p*-ClC_6H_4	2	83	$C_{15}H_{12}ClN_3O_4$	34.83 (27.99−43.35)
5i	*p*-ClC_6H_4	3	81	$C_{16}H_{14}ClN_3O_4$	10.37 (8.05−13.36)
5j	*p*-$NO_2C_6H_4$	1	38[d]	$C_{14}H_{10}N_4O_6$	4.76 (3.61−6.27)
5k	*m*-$NO_2C_6H_4$	1	61	$C_{14}H_{10}N_4O_6$	4.46 (3.55−5.60)
5l	*o*-$NO_2C_6H_4$	1	26[d]	$C_{14}H_{10}N_4O_6$	6.06 (4.60−7.99)
5m	C_6H_5	4	65	$C_{17}H_{17}N_3O_4$	28.37 (23.06−34.90)
Sorbinil					3.04 (2.35−3.93)

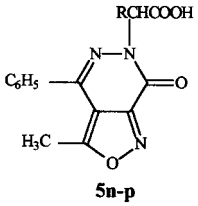

5n-p

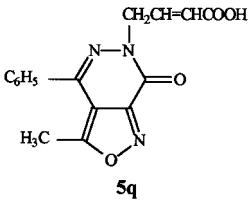

5q

compd	R	yield %[a]	formula[b]	ALR2 inhibition[c]
5n	CH_3	52	$C_{15}H_{13}N_3O_4$	76.84 (59.51−99.22)
5o	CH_2CH_3	44	$C_{16}H_{15}N_3O_4$	75.15 (60.66−93.09)
5p	$CH_2CH_2CH_3$	53	$C_{17}H_{17}N_3O_4$	114 (86−151)
5q		74	$C_{16}H_{13}N_3O_4$	107 (87−132)

[a] From the corresponding **2**. [b] All compounds had C, H, and N microanalysis within ±0.4 of the theoretical value. [c] IC_{50} (μM) (95% CL) or percent inhibition (at a given concentration). [d] From **5a**.

Table 2. Structural and Biological Properties of Compounds **6a**−**d**

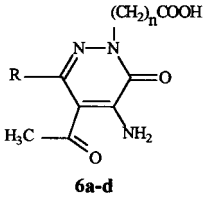

6a-d

compd	R	*n*	yield %[a]	formula[b]	ALR2 inhibition[c]
6a	C_6H_5	1	48	$C_{14}H_{13}N_3O_4$	154 (122−194)
6b	C_6H_5	2	66	$C_{15}H_{15}N_3O_4$	27% (142 μM)
6c	C_6H_5	3	58	$C_{16}H_{17}N_3O_4$	37.01 (30.78−44.49)
6d	CH_3	1	53	$C_9H_{11}N_3O_4$	210 (159−278)
Sorbinil					3.04 (2.35−3.93)

[a] From the corresponding **3**. [b] All compounds had C, H, and N microanalysis within ±0.4 of the theoretical value. [c] IC_{50} (μM) (95% CL) or percent inhibition (at a given concentration).

pyridazinone ring hydrogen bonds to Cys298. The pyridazinone ring makes favorable contacts with the Trp20 side chain, and the isoxazole ring is in contact with the Trp128 side chain. The methyl substituent of the isoxazole ring is in van der Waals contact with the hydrophobic side chain of Leu300. The *p*-chlorophenyl substituent of **5g** interacts favorably with the Phe122 and Pro218 side chains. Noteworthy, the compound in which the *p*-chlorophenyl substituent is replaced by a methyl group (compound **5d**) is considerably less active than **5g**, probably because of less attractive interactions with Phe122 and Pro218.

To highlight the analogies between the structure of the complex of inhibitor **5g** with ALR2 and the structures of the complexes of benzocinnolinone carboxylic acid inhibitors previously reported,[5,12] their structures have been superimposed in Figure 2. As can be evidenced from the superimposition, the carboxylate of all inhibitors occupies very similar positions, interacting with Tyr48, His110, and Trp111. Inhibitors also have in common the ability to hydrogen bond with Cys298. The isoxazole ring of **5g** slightly protrudes toward Leu300 with respect to the benzocinnolinone carboxylic acid inhibitor, while the *p*-chlorophenyl substituent is well superimposed with the terminal benzene ring of the benzocinnolinone derivative. Therefore, inhibitor **5g** can structurally replace the benzocinnolinone inhibitors, being able to give interactions with nearly the same active site residues. However, **5g** is not evidently able to give interactions in the region of the active site occupied by the benzothiazole ring of **1a**, where conformational changes of the enzyme associated with binding of hydrophobic aromatic substituents proved to afford a considerably more active inhibitor than **1**.[12] The insertion of a benzothiazolylmethyl group at position 4 of substrates **6**−**8** would possibly give more active

Table 3. Structural and Biological Properties of Compounds **7a**−**g**

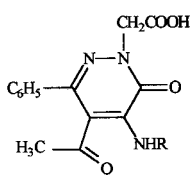

7a-f

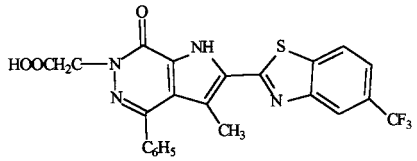

7g

compd	R	yield %[a]	formula[b]	ALR2 inhibition[c]
7a	C_6H_5	40	$C_{20}H_{17}N_3O_4$	12% (16 μM)
7b	$CH_2C_6H_5$	53	$C_{21}H_{19}N_3O_4$	27.60 (22.28−34.19)
7c	$CH_2CH_2C_6H_5$	38	$C_{22}H_{21}N_3O_4$	93.89 (76.67−115)
7d	*p*-ClC_6H_4	63	$C_{20}H_{16}ClN_3O_4$	27% (94 μM)
7e	*p*-BrC_6H_4	60	$C_{20}H_{16}BrN_3O_4$	133 (111−159)
7f	$CH_2C_6H_4Cl$-*p*	49	$C_{21}H_{18}ClN_3O_4$	36.45 (28.95−45.89)
7g		53	$C_{23}H_{15}FN_4O_3S$	97.93 (79.60−120.5)
Sorbinil				3.04 (2.35−3.93)

[a] From the corresponding **9**. [b] All compounds had C, H, and N microanalysis within ±0.4 of the theoretical value. [c] IC_{50} (μM) (95% CL) or percent inhibition (at a given concentration).

Table 4. Structural and Biological Properties of Compounds **8a**−**d**

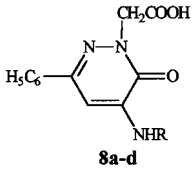

8a-d

compd	R	yield %[a]	formula[b]	ALR2 inhibition[c]
8a	H	70	$C_{12}H_{11}N_3O_3$	36% (82 μM)
8b	$CH_2C_6H_5$	45	$C_{19}H_{17}N_3O_3$	48.82 (40.89−58.29)
8c	$CH_2CH_2C_6H_5$	41	$C_{20}H_{19}N_3O_3$	68.47 (54.51−86.00)
8d	CH_2CH_2-pyridyl-2	36	$C_{19}H_{18}N_4O_3$	157 (122−202)
Sorbinil				3.04 (2.35−3.93)

[a] From the corresponding **15**. [b] All compounds had C, H, and N microanalysis within ±0.4 of the theoretical value. [c] IC_{50} (μM) (95% CL) or percent inhibition (at a given concentration).

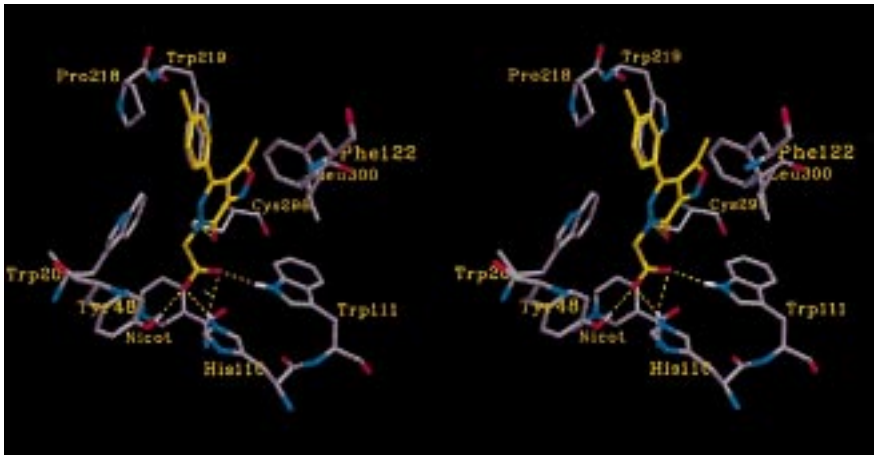

Figure 1. Selection of residues interacting with the inhibitor **5g** (yellow) in the structure of the minimized complex with ALR2 (stereoview). Hydrogen bonds are drawn as dashed lines.

inhibitors, since such a substituent would probably fit ALR2 in a very similar way to that of **1a**. Several attempts to introduce this moiety have been done without success. Further studies are in progress to reach this target.

Conclusion

A number of derivatives (**5**−**8**) were synthesized and tested for their inhibiting properties against aldose reductase, in comparison with the previously reported benzocinnolinone derivative **1**. Several of the bicyclic compounds **5** were found to be provided with properties similar to those of the model. In this series the presence of an electron-withdrawing group on the phenyl at position 4 and of an acetic acid side chain at N-6 led to the most active derivatives (**5g,j**−**l**). On the contrary, elongation of the acidic chain as well as branching or the presence of a double bond proved to be detrimental. All the monocyclic derivatives (**6**−**8**) were found either inactive or very weakly active. Finally, modeling studies

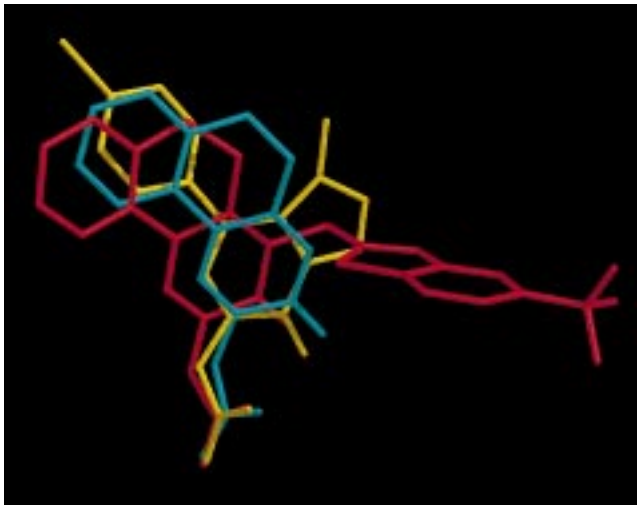

Figure 2. Superimposition of the structures of **5g** (yellow), **1** (cyan), and **1a** (red) bound to ALR2.

performed on the most potent derivative **5g** seem to suggest that this substrate gives very similar interactions with the aldose reductase binding site with respect to the previously reported benzocinnolinone model **1**.

Experimental Section

Chemistry. Melting points were determined on a Büchi 510 capillary melting point apparatus and are uncorrected. Analyses indicated by the symbols were within ±0.4 of the theoretical values. ^{1}H NMR spectra were recorded on a Bruker AC200 spectrometer; chemical shifts are reported as δ (ppm) relative to tetramethylsilane (Table 5). TLC on silica gel plates was used to check product purity. Silica gel 60 (Merck; 70−230 mesh) was used for column chromatography and silica gel 60 (Merck, 230−400 mesh) for flash chromatography.

General Procedure for the Synthesis of the 3-Methyl-4-substituted Isoxazolo-[3,4-*d*]-pyridazin-7-(6*H*)-one-6 Aliphatic Acids (5a−q). A mixture of the required isoxazolo-[3,4-*d*]-pyridazin-7-(6*H*)-one (**2**)[8] (0.01 mol), the appropriate alkyl bromoester (0.02 mol), and potassium carbonate (0.02 mol) in acetone (40 mL) was refluxed overnight. After the mixture cooled, the inorganic salts were filtered off, the solvent was evaporated, and the residue was purifed by flash chromatography to give the esters **9**, which were stirred with sodium hydroxide (0.04 mol) in 95% ethanol (40 mL) at room temperature for 2 h. After evaporation of the solvent, the residue was acidified by hydrochloric acid in diethyl ether, diluted with water (20 mL), and extracted with dichloromethane (3 × 10 mL). After the solvent was dried (Na_2SO_4) and evaporated, the residue was crystallized from ethanol. (See Table 1 for data.)

General Procedure for the Synthesis of the 4-Amino-5-acetyl-6-substituted Pyridazin-3-(2*H*)-one-2 Aliphatic Acids (6a−d). Compounds were prepared as described above for **5a−q**, starting from **3**.[8] (See Table 2 for data.)

General Procedure for the Synthesis of the 5-Acetyl-4-arylamino-6-phenyl Pyridazin-3-(2*H*)-one-2 Acetic Acids (7a−f). (a) To a suspension of **9a** (1.2 mmol) in 50% acetic acid (16 mL) and 65% nitric acid (3.0 mL) cerium ammonium nitrate (CAN, 15 mmol) was added portionwise over a 30 min time. Ice cold water (100 mL) was then added, and the mixture was extracted with dichloromethane (3 × 50 mL). After drying, the solvent was evaporated to give a residue which was purified by silica gel chromatography (eluent toluene/ethyl acetate 8/2) and then crystallized from ethanol to give **10**: yield 38%; mp = 116−118 °C; ^{1}H NMR ($CDCl_3$) δ 1.3 (t, 3H, J = 7.1 Hz), 2.1 (s, 3H), 4.3 (q, 2H, J = 7.1), 5.0 (s, 2H), 7.5 (m, 5H). Anal. ($C_{15}H_{15}N_3O_6$) C, H, N.

(b) A mixture of **10** (0.05 mmol) and the appropriate arylamine (0.15 mmol) in EtOH (15 mL) was stirred for 20 min at room temperature and the so-formed precipitate collected by suction. In the case of an oily ester, the mixture was first diluted with water (8 mL) and then extracted with CH_2Cl_2 (3 × 20 mL). The so-obtained esters **11** were hydrolyzed by hydroalcoholic 2 N NaOH (3 mL) at room temperature for 15−60 min. After concentration of the solvent, the mixture was acidified by 6 N HCl and the so-formed acids **7** were either obtained by suction or by extraction with CH_2Cl_2 (3 × 20 mL). (See Table 3 for data.)

It should be noted that when **10** was condensed with 2-chloro-5-(trifluoromethyl)benzothiazole, the hydrolysis of the corresponding ester (**11g**) led to the unexpected **7g**. (See Scheme 2.)

For **11g**: yield 70%; mp = 74−75 °C; ^{1}H NMR ($CDCl_3$) δ 1.3 (t, 3H, J = 7.0 Hz), 1.8 (s, 3H), 4.2 (q, 2H, J = 7.0 Hz), 4.9 (s, 2H), 5.4 (d, 2H), 7.4 8s, 5H), 7.6 (d, 1H, J = 9.9 Hz), 8.0 (d, 1H, J = 9.9 Hz), 8.3 (s, 1H), 9.1 (br s, 1H, exch with D_2O). Anal. ($C_{25}H_{21}F_3N_4O_4$) C, H, N.

Table 5. ^{1}H NMR Data for the Acids **5−8**

compd	^{1}H NMR[a]
5a	2.6 (s, 3H); 5.0 (s, 2H); 7.6−7.7 (m, 5H)
5b	2.6 (s, 3H); 2.9 (t, 2H, J = 7.8); 4.5 (t, 2H, J = 7.8); 7.6−7.7 (m, 5H)
5c	2.1−2.2 (m, 2H); 2.4 (t, 2H, J = 7.8); 2.6 (s, 3H); 4.3 (t, 2H, J = 7.8); 7.6−7.7 (m, 5H)
5d	2.5 (s, 3H); 2.9 (s, 3H); 4.8 (s, 2H)
5e	2.5 (s, 3H); 2.7 (t, 2H, J = 7.8); 2.9 (s, 3H); 4.3 (t, 2H, J = 7.8)
5f	1.9−2.0 (m, 2H); 2.3 (t, 2H, J = 7.8); 2.5 (s, 3H); 3.0 (s, 3H); 4.0 (t, 2H, J = 7.8)
5g	2.6 (s, 3H); 4.9 (s, 2H); 7.5−7.6 (2d, 4H, J = 9)
5h	2.6 (s, 3H); 2.8 (t, 2H, J = 7.8); 4.2 (t, 2H, J = 7.8); 7.6,7.7 (2d, 4H, J = 9.0)
5i	2.2 (m, 2H); 2.4 (t, 2H, J = 7.8); 2.6 (s, 3H); 4.3 (t, 2H, J = 7.8); 7.5,7.6 (2d, 4H, J = 9.0)
5j	2.6 (s, 3H); 4.6 (s, 2H); 8.0, 8.4 (2d, 4H, J = 10)
5k	2.6 (s, 3H); 4.9 (s, 2H); 8.0 (m, 2H); 8.4 (m, 2H)
5l	2.4 (s, 3H); 4.5 (s, 2H); 7.9 (m, 2H); 8.3 (m 1H); 8.4 (m, 1H)
5m	1.5−1.9 (m, 4H); 2.3 (t, 2H, J = 7.8); 2.6 (s, 3H); 4.1 (t, 2H, J = 7.8); 7.6−7.7 (m, 5H)
5n	1.7 (d, 3H, J = 7.5); 2.7 (s, 3H); 5.7 (q, 1H, J = 7.5); 7.6−7.8 (m, 5H)
5o	1.2−1.4 (m, 2H); 1.6 (t, 3H, J = 7.6); 2.6 (s, 3H); 5.6 (t, 1H, J = 7.6); 7.5−7.7 (m, 5H)
5p	0.9 (t, 3H, J = 7.6); 1.0−1.1 (m, 2H); 2.0−2.1 (m, 2H); 2.5 (s, 3H); 5.5 (t, 1H, J = 7.7); 7.6 (app s, 5H)
5q	2.5 (s, 3H); 4.9 (d, 1H); 5.9 (d, 1H); 7.0−7.2 (m, 1H); 7.4−7.6 (m, 5H)
6a	1.8 (s, 3H); 4.8 (s, 2H); 7.4−7.6 (m, 5H)
6b	1.8 (s, 3H); 2.8 (t, 3H, J = 7.5); 4.3 (t, 2H, J = 7.5); 7.4−7.6 (m, 5H)
6c	1.8 (s, 3H); 2.0−2.2 (m, 2H); 2.5 (t, 2H, J = 7.5); 4.3 (t, 2H, J = 7.5); 7.4−7.6 (m 5H)
6d	1.8 (s, 3H); 2.9 (s, 3H); 4.8 (s, 2H)
7a	1.6 (s, 3H); 5.0 (s, 2H); 7.1−7.2 (m, 5H); 7.3−7.4 (m, 5H)
7b	1.6 (s, 3H); 4.7 (d, 2H, J = 6.2); 5.0 (s, 2H); 7.2−7.3 (m, 5H); 7.4 (app s, 5H)
7c	1.8 (s, 3H); 2.9 (t, 2H, J = 7.0); 3.7−3.8 (m, 2H); 4.9 (s, 2H); 7.2−7.3 (m, 5H); 7.4 (app s, 5H)
7d	1.7 (s, 3H); 5.5 (s, 2H); 7.0 (d, 2H, J = 9); 7.2 (d, 2H, J = 9.0); 7.4 (app s, 5H)
7e	1.8 (s, 3H); 5.0 (s, 2H); 7.0 (d, 2H, J = 8.1); 7.3−7.4 (m, 7H)
7f	1.5 (s, 3H); 4.7 (d, 2H, J = 6.3); 5.0 (s, 2H); 7.1 (d, 2H, J = 8.2); 7.3 (d, 2H, J = 8.2); 7.4 (app s, 5H)
8a	4.8 (s, 2H); 5.8 (s, 2H); 6.7 (s, 1H); 7.3−7.5 (m, 3H); 7.7−7.9 (m, 2H)
8b	4.6 (d, 2H, J = 6.3); 4.8 (s, 2H); 6.6 (s, 1H); 7.2−7.4 (m, 8H); 7.7−7.9 (m, 2H)
8c	3.0 (t, 2H, J = 7.5); 3.4−3.5 (m, 2H); 4.8 (s, 2H); 6.7 (s, 1H); 7.1−7.6 (m, 8H); 7.8−8.0 (m, 2H)
8d	3.7 (t, 2H, J = 7.5); 4.0−4.1 (m, 2H); 5.3 (s, 2H); 6.8 (s, 1H); 7.1−7.5 (m, 5H); 7.6 (t, 1H); 7.8−8.0 (m, 2H); 8.4−8.6 (m, 1H)

For **7g**: yield 53%; mp > 300 °C; ^{1}H NMR ($CDCl_3$) δ 2.2 (s, 3H), 3.3 (br s, 1H, exch with D_2O), 4.9 (s, 2H), 7.6−7.7 (m, 6H), 8.3−8.4 (m, 2H). Anal. ($C_{23}H_{15}F_3N_4O_3S$) C, H, N, S.

General Procedure for the Synthesis of the 4-(Substituted)amino-6-phenyl-pyridazin-3-(2*H*)-one-2 Acetic Acids (8a−d). A mixture of the known **13**[11] (0.13 g; 0.57 mmol) and the required amine (2.5 mmol) in ethanol (5 mL) was refluxed overnight. The residue was then purified by flash chromatography (cyclohexane/ethyl acetate 95/5) to give **14**, which was refluxed with acetic acid (1 mL). After cooling and alkalinization to pH 8 by diluted sodium hydroxide, the aminopyridazinones **15** were extracted by CH_2Cl_2. After drying over sodium sulfate and evaporation of the solvent, the crude residue was used as such for the next step. The esters **16** and their corresponding acids **8** were easily obtained as described above for **5**. (See Table 4 for data.)

Enzyme Section. (+)-(*S*)-6-Fluoro-2,3-dihydrospiro-(4H-1-benzopyran-4,4′-imidazolidine)-2′,5′-dione (Sorbinil) was a gift from Pfizer (Groton, CT). Calf lenses for the purification of Aldose reductase (ALR2, alditol:NADP+ oxidoreductase, EC 1.1.1.21) were obtained locally from freshly slaughtered animals. The capsule was incised, and the frozen lens was suspended in sodium potassium phosphate buffer, pH 7 (standard buffer), containing 5 mM DTT (1 g tissue/3.5 mL) and stirred in an ice cold bath for 1 h. The suspension was then centrifuged at 22000*g* at 4 °C for 40 min, and the supernatant was subjected to ion exchange chromatography on DE52, affinity chromatography on Orange MatrexA, and to Sephadex G75 chromatography, as previously described.[5] Enzyme activity for all tested enzymes was measured by monitoring the change in absorbance at 340 nm which accompanies the oxidation of NADPH catalyzed by ALR2. The assay was performed at 37 °C as previously described,[5] using 4.7 mM D,L-glyceraldehyde as substrate in 0.25 M sodium phosphate buffer, pH 6.8, containing 0.38 M ammonium sulfate and 0.11 mM NADPH. The sensitivity of the enzymes to inhibition by different ARIs and newly synthesized compounds was tested in the above assay conditions by including the inhibitor dissolved in DMSO at the desired concentration in the reaction mixture. DMSO in the assay mixture was kept at constant concentration of 1%. A reference blank containing all the above reagents except the substrate was used to correct for the nonenzymatic oxidation of NADPH. IC_{50} values (the concentration of the inhibitor required to produce 50% inhibition of the enzyme catalyzed reaction) were determined from least squares analyses of the linear portion of the log dose−inhibition curves. Each curve was generated using at least three concentrations of inhibitor causing an inhibition between 20% and 80% with two replicates at each concentration. The 95% confidence limits (95% CL) were calculated from *T* values for $n - 2$, where n is the total number of determinations.[13]

Computational Procedure. Molecular mechanics simulations were performed using the AMBER4.1[14] program with the Cornell et al.[15] force field on SGI O2 computers. Graphic display was performed with MIDAS.[16] The geometry of inhibitor **5g** was completely optimized using the AM1 Hamiltonian. Parameters for **5g** were set consistently to the Cornell et al.[15] force field. Missing bond and angle parameters were assigned on the basis of analogy with known parameters in the database and calibrated to reproduce the AM1 optimized geometry. The partial charges on atoms of **5g** were calculated from an electrostatic potential fit to a 6-31G* ab initio wave function using Gaussian94, followed by RESP analysis.[17,18] Parameters for $NADP^+$ were taken from our previous simulations.[5,12] The crystal structure coordinates of the human ALR2 holoenzyme[6] were used. The carboxylate group of the inhibitor **5g** was initially positioned to interact with the nicotinamide ring of $NADP^+$ and with the nearby residues, as indicated by the binding of other carboxylic acid inhibitors[6,7] and previous modeling results.[5,12] Three thousand steps of conjugate gradient minimization were performed. All protein residues within 10 Å from the inhibitor were allowed to move during minimization. A distance-dependent dielectric constant with a 4*r* dependence and 10 Å nonbonded cutoff were adopted.

References

(1) Porte, D., Jr.; Schwartz, M. W. Diabetic complications: Why is glucose potentially toxic? *Science* **1996**, *272*, 699−700.

(2) Tomlinson, D. R.; Stevens, E. J.; Diemel, L. Aldose reductase inhibitors and their potential for the treatment of diabetic complications. *Trends Pharmacol. Sci.* **1994**, *15*, 293−297.

(3) Kador, P. F. The role of aldose reductase in the development of diabetic complications. *Med. Res. Rev.* **1988**, *8*, 325−352.

(4) Pfeifer, M. A.; Schumer, M. P.; Gelber, D. A. Aldose reductase inhibitors: The end of an era or the need of different trial designs? *Diabetes* **1997**, *46*, Suppl. 2, S82−S89.

(5) Costantino, L.; Rastelli, G.; Vescovini, K.; Cignarella, G.; Vianello, P.; Del Corso, A.; Cappiello, M.; Mura, U.; Barlocco, D. Synthesis, activity and molecular modeling of a new series of tryciclic pyridazinones as selective aldose reductase inhibitors. *J. Med. Chem.* **1996**, *39*, 4396−4405.

(6) Wilson, D. K.; Tarle, I.; Petrash, J. M.; Quiocho, F. A. Refined 1.8 Å structure of human aldose reductase complexed with the protein inhibitor zopolrestast. *Proc. Natl. Acad. Sci. U.S.A.* **1993**, *90*, 9847−9851.

(7) Urzhumtsev, A.; Tete-Favier, F.; Mitschler, A.; Barbanton, J.; Barth, P.; Urzhumtseva, L.; Biellmann, J. F.; Podjarni, A. D.; Moras, D. U. A "specificity" pocket inferred from the crystal structures of the complexes of aldose reductase with the pharmaceutically important inhibitors tolrestat and sorbinil. *Structure* **1997**, *5*, 601−612.

(8) Dal Piaz, V.; Ciciani, G.; Turco, G.; Giovannoni, M. P.; Miceli, M.; Pirisino, R.; Perretti, M. 5-Acyl-6-aryl-4-nitro-3(2*H*)-pyridazinones and related 4-amino compounds: Synthesis and pharmacological evaluation. *J. Pharm. Sci.* **1991**, *80*, 341−348.

(9) Mylari, B. L.; Larson, E. R.; Beyer, T. E.; Zembrowski, W. J.; Aldinger, C. E.; Dee, M. F.; Siegel, T. W.; Singleton, D. H. Novel, potent aldose reductase inhibitors: 3,4-dihydro-4-oxo-3[(5-(trifluoromethyl)2-benzothiazolylmethyl]-1-phthalazineacetic acid (Zopolrestat) and congeners. *J. Med. Chem.* **1991**, *34*, 108−122.

(10) Aotsuka, T.; Abe, N.; Fukushima, K.; Ashizawa, N.; Yoshida, M. Benzothiazol-2-yl-carboxylic acids with diverse spacers: A novel class of potent, orally active aldose reductase inhibitors. *Bioorg. Med. Chem. Lett.* **1997**, *7*, 1677−1682.

(11) Sircar, I. Synthesis of 4-amino-6-phenyl-3(2*H*)-pyridazinones: a general procedure. *J. Heterocyclic Chem.* **1983**, *20*, 1473−1476.

(12) Rastelli, G.; Vianello, P.; Barlocco, D.; Costantino, L.; Dal Corso, A.; Mura U. Structure-based design of an inhibitor modeled at the substrate active site of aldose reductase. *Bioorg. Med. Chem. Lett.* **1997**, *7*, 1897−1902.

(13) Tallarida, R. J.; Murray, R. B. *Manual of Pharmacologic calculations with computer programs*, 2nd ed.; Springer-Verlag: New York, 1987.

(14) Pearlman, D. A.; Case, D. A.; Caldwell, J. W.; Ross, W. S.; Cheatman, T. E., III; Ferguson, D. M.; Seibel, G. L.; Singh, U. C.; Weiner, P. K.; Kollman, P. A. *AMBER 4.1*; University of California: San Francisco, 1995.

(15) Cornell, W. D.; Cieplak, P.; Bayly, C. I.; Gould, I. R.; Merz, K. M., Jr.; Ferguson, D. M.; Spellmeyer, D. C.; Fox, T.; Caldwell, J. W.; Kollman, P. A. A second generation force field for the simulation of proteins, nucleic acids, and organic molecules. *J. Am. Chem. Soc.* **1995**, *117*, 5179−5197.

(16) Ferrin, T. E.; Huang, C. C.; Jarvis, L. E.; Langrifge, R. J. The MIDAS display system. *Mol. Graphics* **1988**, *6*, 13−27.

(17) Bayly, C. I.; Cieplak, P.; Cornell, W. D.; Kollman, P. A. A well-behaved electrostatic potential based method using charge restraints for deriving atomic charges: The RESP model. *J. Phys. Chem.* **1993**, *97*, 10269−10280.

(18) Cieplak, P.; Bayly, C. I.; Cornell, W. D.; Kollman, P. A. Application of the multimolecule and multiconformational RESP methodology to biopolymers: charge derivation for DNA, RNA and proteins. *J. Comput. Chem.* **1995**, *16*, 1357−1377.

JM981107O